environmental microbiology

Environmental Microbiology (2022) **24**(5), 2259–2269 doi:10.1111/1462-2920.15877

Dissolved organic phosphorus utilization by the marine bacterium *Ruegeria pomeroyi* DSS-3 reveals chain length-dependent polyphosphate degradation

Jamee C. Adams [1], **Rachel Steffen**,[2,3] **Chau-Wen Chou**,[4] **Solange Duhamel** [5] and **Julia M. Diaz** [1,2*]

[1]*Geosciences Research Division, Scripps Institution of Oceanography, University of California San Diego, La Jolla, CA, 92093.*

[2]*Department of Marine Sciences, Skidaway Institute of Oceanography, University of Georgia, Savannah, GA, 31411.*

[3]*Department of Marine Sciences, University of Georgia, Athens, GA, 30602.*

[4]*Proteomics and Mass Spectrometry Core Facility, University of Georgia, Athens, GA, 30602.*

[5]*Department of Molecular and Cellular Biology, The University of Arizona, Tucson, AZ, 85721.*

Summary

Dissolved organic phosphorus (DOP) is a critical nutritional resource for marine microbial communities. However, the relative bioavailability of different types of DOP, such as phosphomonoesters (P-O-C) and phosphoanhydrides (P-O-P), is poorly understood. Here we assess the utilization of these P sources by a representative bacterial copiotroph, *Ruegeria pomeroyi* DSS-3. All DOP sources supported equivalent growth by *R. pomeroyi*, and all DOP hydrolysis rates were upregulated under phosphorus depletion (−P). A long-chain polyphosphate (45polyP) showed the lowest hydrolysis rate of all DOP substrates tested, including tripolyphosphate (3polyP). Yet the upregulation of 45polyP hydrolysis under −P was greater than any other substrate analyzed. Proteomics revealed three common P acquisition enzymes potentially involved in polyphosphate utilization, including two alkaline phosphatases, PhoD and PhoX, and one 5′-nucleotidase (5′-NT). Results from DOP substrate competition experiments show that these enzymes likely have broad substrate specificities, including chain length-dependent reactivity toward polyphosphate. These results confirm that DOP, including polyP, are bioavailable nutritional P sources for *R. pomeroyi*, and possibly other marine heterotrophic bacteria. Furthermore, the chain-length dependent mechanisms, rates and regulation of polyP hydrolysis suggest that these processes may influence the composition of DOP and the overall recycling of nutrients within marine dissolved organic matter.

Received 3 September, 2021; revised 16 November, 2021; accepted 14 December, 2021. *For correspondence. E-mail j2diaz@ucsd.edu.

Introduction

Phosphorus (P) is a fundamental nutrient for all living organisms. While inorganic phosphate (Pi) is considered the preferred form of P, the capacity to utilize dissolved organic phosphorus (DOP) provides marine microorganisms with the ability to thrive in regions where low Pi concentrations may otherwise preclude significant growth, particularly in oligotrophic regions where DOP comprises the majority of the total dissolved P pool (Karl, 2014; Karl and Björkman, 2015; Duhamel *et al*., 2021). Yet DOP utilization supports microbial P nutritional requirements even in coastal and nutrient-replete regions, including areas with excess nitrogen due to nutrient overloading (Dyhrman and Ruttenberg, 2006; Lin *et al*., 2016; Davis and Mahaffey, 2017), making DOP a critical resource across diverse marine habitats. Indeed, microbial DOP utilization supports primary productivity, nitrogen fixation and carbon export on global and regional scales (Duhamel *et al*., 2021). Furthermore, microbial DOP degradation helps control the composition of dissolved organic matter (DOM) by driving the preferential remineralization of P (Letscher and Moore, 2015). However, the relative utilization of different types of DOP is not completely understood.

DOP is commonly categorized into three major bond classes. First, phosphoesters (P-esters) contain one (monoester) or two (diester) P-O-C bonds and make up approximately 80% of total (high + low molecular weight) marine DOP (Young and Ingall, 2010). Highly labile P-monoesters include adenosine monophosphate (AMP)

and adenosine triphosphate (ATP), which both contain an alpha Pi group linked to the adenosine structure (Moore *et al*., 2005; Dyhrman and Ruttenberg, 2006; Diaz *et al*., 2018). Next, phosphonates contain a direct C-P bond and account for approximately 10% of marine DOP (Young and Ingall, 2010). Finally, phosphoanhydrides (P-anhydrides) contain P-O-P bonds and make up the final ~10% of marine DOP (Young and Ingall, 2010). P-anhydrides include inorganic polyphosphate (polyP), as well as organic compounds such as ATP, which has P-anhydride bonds linking the alpha-beta and the beta-gamma Pi groups. Inorganic polyP is a polymer consisting of at least three and up to thousands of Pi molecules, which is made by every cell in nature (Kornberg *et al*., 1999) and is ubiquitous in the marine environment (Paytan *et al*., 2003; Sannigrahi and Ingall, 2005; Diaz *et al*., 2008; Martin *et al*., 2014; Diaz *et al*., 2016; Martin *et al*., 2018). A common method for quantifying polyP (Martin and Van Mooy, 2013) can only detect chains with at least 15 P atoms (Diaz and Ingall, 2010), suggesting that a substantial fraction of marine polyP is composed of larger polymers (Martin and Van Mooy, 2013; Martin *et al*., 2014, 2018; Diaz *et al*., 2016).

Each DOP bond class is bioavailable to some degree (Björkman and Karl, 2005; Martin *et al*., 2014, 2018; Sosa *et al*., 2020). For example, P-ester utilization is widespread across prokaryotic and eukaryotic plankton and is thought to be driven mainly by the enzyme alkaline phosphatase (AP) (Duhamel *et al*., 2021), which is usually assumed to target only P-O-C bonds. On the other hand, phosphonate utilization is generally regarded as a prokaryotic process (Cui *et al*., 2016; Repeta *et al*., 2016; Sosa *et al*., 2020), with some exceptions (Wang *et al*., 2016; Whitney and Lomas, 2019), and includes mechanisms such as the C-P lyase pathway (Sosa *et al*., 2019). PolyP is bioavailable to eukaryotic phytoplankton (Diaz *et al*., 2016, 2019), cyanobacteria (Moore *et al*., 2005) and natural marine microbial communities (Benitez-Nelson and Buesseler, 1999; Alexander *et al*., 2015; Nausch *et al*., 2018); however, mechanisms of polyP utilization are generally unknown. The enzyme 5′-nucleotidase (5′-NT) is widespread in the ocean and targets both P-ester and P-anhydride bonds through the degradation of nucleotides (Ammerman and Azam, 1985). However, whether 5′-NT is involved in inorganic polyP degradation remains unclear. Additionally, very little is known about the cycling of marine polyP with varying chain lengths.

In order to expand our understanding of polyP bioavailability and cycling in the context of other labile DOP sources, we examined the utilization of representative P-esters and P-anhydrides by the marine heterotrophic bacterium *Ruegeria pomeroyi* DSS-3. *R. pomeroyi* belongs to the *Roseobacter* clade of Alphaproteobacteria, which can represent up to 30% of marine bacterial communities (Buchan *et al*., 2005). Furthermore, *R. pomeroyi* is a representative copiotroph of coastal and carbon-rich environments where DOP is dynamically cycled and can contribute to microbial P demand, even when Pi is available (Benitez-Nelson and Buesseler, 1999; Nausch *et al*., 2018). Here we examine the relative preferences of *R. pomeroyi* for P-esters (e.g. AMP, ATP) and P-anhydrides (ATP, 3polyP, 45polyP) under Pi-replete (+Pi) and P-depleted (−P) conditions. Additionally, we conducted proteomic analysis and DOP substrate competition experiments to identify enzymes that are likely to be involved in the degradation of polyP. Overall, results show that the mechanisms, rates and regulation of polyP utilization are chain length-dependent, yet polyP supports similar levels of growth as highly labile P-monoesters, regardless of chain length. These findings have implications for DOP composition and dynamics as well as microbial nutritional physiology.

Results

Growth on alternative P sources

In order to test the ability of *R. pomeroyi* to grow on different forms of DOP, representative P-esters or P-anhydrides were provided as P sources in culture media. Based on daily optical density (OD), final cell concentrations and growth rates, all model DOP sources supported the same level of growth by *R. pomeroyi* as Pi (Fig. 1). As a control, we grew cultures in −P media. These −P cultures confirmed a substantial lack of growth when compared to cultures provided with Pi or DOP. This finding confirms that the growth observed in DOP-amended cultures was indeed due to growth on DOP, rather than on any other P source present in the media. Final cell counts were observed following the plateau in OD values during stationary phase. Final cell counts were ~3–4 $\times 10^8$ cells ml^{-1} for +Pi and +DOP cultures, and ~1 $\times 10^7$ cells ml^{-1} for −P cultures. Growth rates were 0.2 h^{-1} for +Pi and +DOP cultures, and 0.1 h^{-1} for −P cultures. Pi concentrations in +Pi cultures decreased over the course of growth from 18 μM (starting media concentration) to ~1.7 μM (midlog, T4), and were below detection (<800 nmol L^{-1}) by stationary phase (T7).

DOP hydrolysis

DOP hydrolysis rates were quantified based on the conversion of model DOP substrates to Pi (fmol Pi $cell^{-1}$ h^{-1}). DOP hydrolysis was measured during midlog and stationary phase in +Pi and −P cultures. In addition, DOP hydrolysis was measured in a subset of culture samples that were filtered (0.2 μm) to partially isolate any

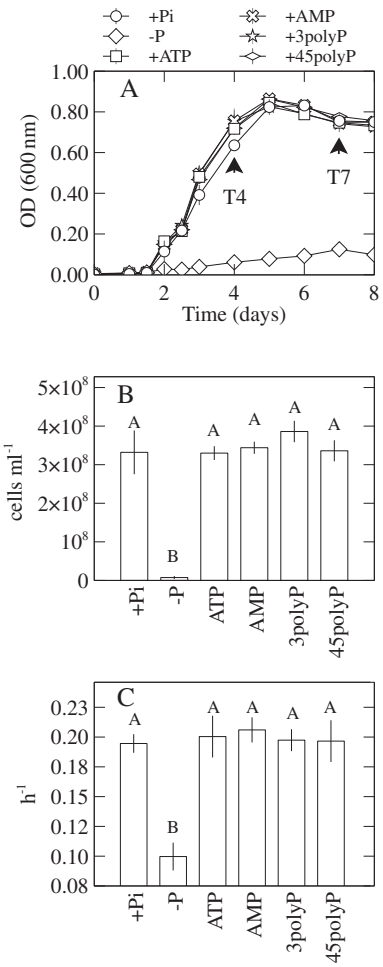

Fig. 1. *Ruegeria pomeroyi* growth on phosphoester and phosphoanhydride substrates.
A. Growth curve represented by changes in optical density over time. Arrows show time of sampling at midlog (T4) and stationary phase (T7) for subsequent analysis.
B. Final cell yield (T7).
C. Growth rates. Error bars indicate one standard deviation of the mean of three biological replicates. P sources lacking a shared letter are significantly different ($p < 0.05$) (ANOVA with Tukey HSD *post hoc* test).

cell-free P-hydrolase enzymes present. All DOP substrates were degraded during both growth phases and in each media type (Fig. 2). Removing the cells by filtration substantially decreased the hydrolysis rates by ~97% (±~4%), which is consistent with the majority of P-hydrolase enzymes being cell-associated (Fig. 2). However, the filtered cultures, or filtrates, still showed measurable levels of DOP hydrolysis (Fig. 2B and D), suggesting that some cell-free P-hydrolases were present, likely due to a combination of processes, including release from cells during filtration, and natural production. DOP hydrolysis rates increased in filtrates during stationary phase compared to mid log (Fig. 2B and D), consistent with an enhanced degradation of cells and/or upregulation of enzymes due to elevated P stress.

The cultures exhibited signs of increasing P stress going into stationary phase and as a function of media type. For example, in midlog growth phase, DOP hydrolysis rates in the whole culture were similar in +Pi and −P cultures (Fig. 2A, S1), however, by the time the cultures reached stationary phase, DOP hydrolysis was significantly higher in −P than +Pi cultures (Fig. 2C). The degree to which the hydrolysis of each DOP source was upregulated as a function of P status was assessed by normalizing the hydrolysis rate of −P treatments to that of +Pi treatments (fold change) in stationary phase. Based on this analysis, long-chain polyphosphate (45polyP) hydrolysis was upregulated much more (~sixfold) in the whole culture than any other DOP source (<threefold; Fig. 3A).

To determine potential DOP substrate preferences, we normalized the hydrolysis rate of each DOP source to the hydrolysis rate of AMP measured at the same time and in the same media type (Fig. 4A). This analysis revealed that most DOP sources were utilized to a similar degree as AMP (~75%–80% of AMP rate), except for 45polyP, which was hydrolyzed significantly less, at only ~40% of the rate of AMP ($p < 0.05$). This result suggests that although 45polyP hydrolysis was the most highly upregulated, 45polyP was the least preferred DOP source overall. Despite being the least preferred DOP source, 45polyP still supported the full growth demand of *R. pomeroyi* (Fig. 1B). Assuming a cell quota of 0.08–0.24 fmol P cell^{-1} under replete conditions (Zimmerman *et al*., 2014; Posacka *et al*., 2019), and the growth rates measured during growth on DOP (~0.2 h^{-1}), the cellular P demand was between ~0.02–0.05 fmol Pi cell^{-1} h^{-1}. These cellular P assimilation rates are lower than all of the DOP hydrolysis rates measured (~0.08–0.16 fmol Pi cell^{-1} h^{-1}), including 45polyP (Fig. 2A and B), confirming that all DOP hydrolysis rates were sufficient to sustain the observed levels of growth.

Proteomics: extracellular P hydrolases

The degradation of DOP sources in filtered cultures (Fig. 2B and D) suggests the presence of cell-free P-hydrolases involved in nutritional DOP utilization. In order to identify these enzymes, proteomic analysis of cell-free filtrates was performed in stationary phase. We observed several expected enzymes that have known roles in microbial DOP utilization: the APs PhoX and PhoD, and 5′-NT. Abundances of each of these P-hydrolases were significantly upregulated under −P compared to +Pi conditions (Fig. 5), which is consistent with DOP hydrolysis rates (Fig. 2B–D). The full exoproteome did not reveal any other enzymes with putative phosphatase activity nor

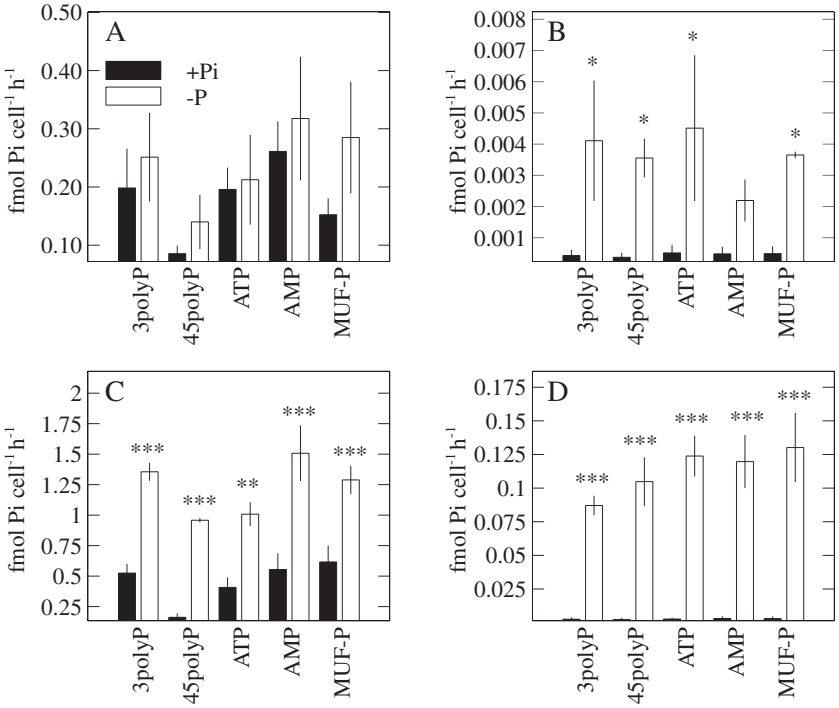

Fig. 2. Hydrolysis rates of DOP sources in +Pi and −P cultures. Whole culture (A, C) and cell-free filtrate (B, D) in midlog (A, B) and stationary phase (C, D). In the case of cell-free filtrates, hydrolysis rates are normalized to the cell abundance determined prior to filtering the cultures. Error bars indicate one standard deviation of the mean of three biological replicates. Significant differences between +Pi and −P conditions are represented by stars above bars: $p < 0.05$ (*), $p < 0.0002$ (**), $p < 0.0001$ (***) (ANOVA with Tukey HSD *post hoc* test).

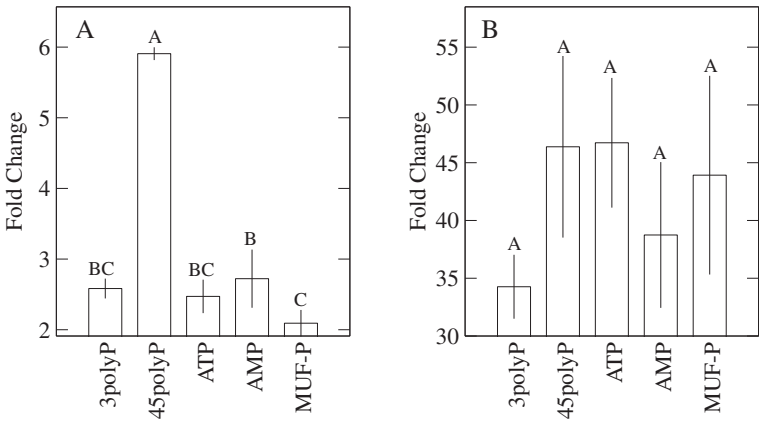

Fig. 3. Degree of DOP hydrolysis upregulation calculated from cell-normalized rates, under −P conditions during stationary phase for (A) whole culture and (B) cell-free filtrate. Error bars indicate one standard deviation of the mean of three biological replicates. P sources lacking a shared letter are significantly different ($p < 0.05$) (ANOVA with Tukey HSD *post hoc* test).

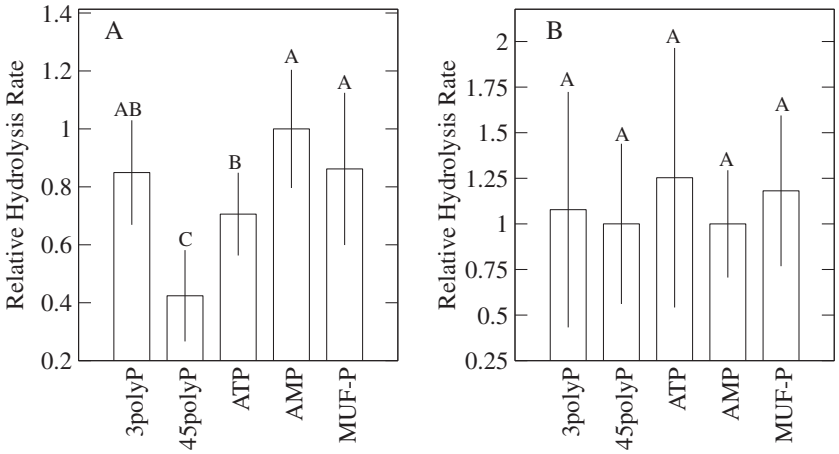

Fig. 4. Relative DOP hydrolysis rates in (A) whole cultures and (B) cell-free filtrates. The hydrolysis rate of each DOP source was normalized to the hydrolysis rate of AMP. Error bars indicate one standard deviation of the mean of three biological replicates. P sources lacking a shared letter are significantly different ($p < 0.05$) (ANOVA with Tukey HSD *post hoc* test).

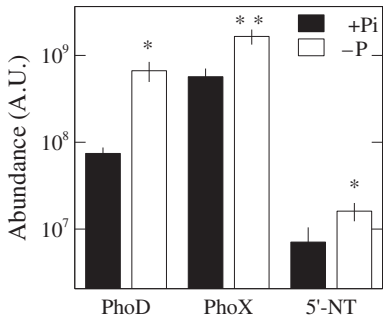

Fig. 5. Average protein abundances (A.U.) in +Pi and −P cell-free filtrates in stationary phase. Error bars indicate one standard deviation of the mean of three biological replicates. Significant upregulation under −P condition represented by stars above bars $p < 0.05$ (*), $p < 0.01$ (**) (Student's *t*-test).

did it reveal any intracellular canonical polyP enzymes like polyphosphate kinase (ppk1 or ppk2) and exopolyphosphatase (ppx) (Dataset S1), which are present in the *R. pomeroyi* genome (Table S1).

APA substrate versatility

In order to assess the substrate versatility of *R. pomeroyi* P-hydrolases, we measured alkaline phosphatase activity (APA) in whole cultures and cell-free filtrates with the addition of competing DOP substrates. APA was measured from the hydrolysis of the fluorogenic probe methylumbelliferyl phosphate (MUF-P), and any inhibition of MUF-P hydrolysis by another DOP source reflected competition for the enzyme active site. Results from these competition experiments showed that all tested DOP sources inhibited MUF-P hydrolysis in a concentration-dependent fashion. Across growth phases, media types, and in whole cultures and cell-free filtrates, AMP showed the greatest inhibition of MUF-P hydrolysis, while tripolyphosphate (3polyP) showed the least (Fig. 6, S2). ATP and 45polyP had a similar, intermediate inhibiting effect on APA (Fig. 6, S2). Half-maximal inhibitory concentrations (IC_{50}) of each DOP source, which correspond to the molecular concentration of substrate responsible for 50% inhibition of MUF-P hydrolysis, were consistent with these trends and exhibited values ranging from ~1.6 to 7.5 μM (Fig. S3). Finally, Pi also inhibited APA in whole cultures and cell-free filtrates (Fig. S4). Stationary phase samples generally showed a greater sensitivity to DOP inhibition compared with midlog; however, the overall substrate trends remained the same between midlog and stationary phases (Fig. 6, S2).

Discussion

The goal of this study was to assess the relative bioavailability and utilization of model DOP sources, including inorganic polyP of different chain lengths, to the marine bacterium *R. pomeroyi*. Representative molecules from P-ester and P-anhydride bond classes were rapidly hydrolyzed in excess of cellular P demand, resulting in equivalent levels of growth on all P sources. However, beneath these comparable growth trends, results also revealed that the hydrolysis of long-chain polyphosphate (45polyP) by *R. pomeroyi* was unique among all of the other P sources examined. First, 45polyP showed the lowest relative hydrolysis rate among all of the P sources tested (Fig. 4A), indicating that it was the least preferred P source. Despite this status, the hydrolysis of 45polyP exhibited the largest degree of upregulation under −P conditions compared to any other P substrate tested (Fig. 3A), suggesting that the relative affinity for 45polyP is greatly enhanced under P stress. A short-chain polyP source (3polyP) did not show these same trends, suggesting that polyP utilization is chain length-dependent in *R. pomeroyi*.

Microorganisms naturally produce inorganic polyP at a range of chain lengths from three up to thousands of P atoms (Kornberg *et al*., 1999). The range of chain lengths in marine pools of polyP remain largely unknown; however, previous studies have shown that 3polyP is bioavailable to mixed plankton communities (Björkman and Karl, 1994), bacteria-enriched assemblages (White *et al*., 2012), cultures of *Prochlorococcus* and *Synechococcus* (Moore *et al*., 2005) and cultures of eukaryotic phytoplankton (Diaz *et al*., 2016, 2019). Although investigations of long-chain polyP bioavailability are relatively rare, one other study (Diaz *et al*., 2016) documented the ability of the diatom *Thalassiosira oceanica* to use multiple polyP chain lengths as sole P sources, in agreement with current results from *R. pomeroyi* (Fig. 1A). Overall, chain length does not seem to affect microbial growth on polyP, but chain length does impact polyP hydrolysis rates by *R. pomeroyi*. This finding implies that microbial polyP hydrolysis may shape the composition of environmental polyP pools by preferentially targeting different polymer lengths.

Particulate long-chain polyP (>~15 P atoms) is preferentially recycled in the Indian Ocean and Sargasso Sea relative to other organic P sources (Martin *et al*., 2014, 2018). In contrast, we did not observe any preference for polyP by *R. pomeroyi*. Differences between these field studies and our culture work could potentially be explained by a number of factors. For instance, the other environmental P sources measured in these field studies may have been more recalcitrant than our highly labile alternative P substrates accounted for. In addition, the discrepancy may suggest species- versus community-level differences in DOP substrate preferences (niche partitioning). For example, in contrast to *R. pomeroyi*, the diatom *Thalassiosira* spp. preferentially degrades polyP

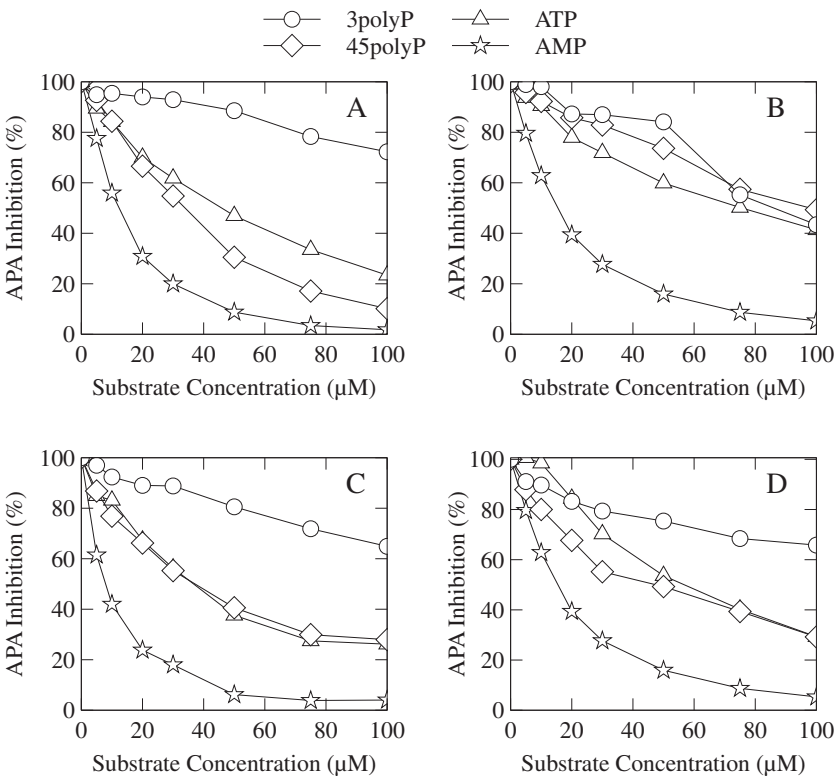

Fig. 6. Concentration-dependent inhibition of APA by competing DOP substrates in stationary phase. Substrate concentrations are in molecular units. Each point represents the average of three biological replicates. Whole culture (A, B) and filtrate (C, D) in +Pi (A, C) and −P (B, D) media. Error bars omitted for clarity. Biological replicates typically agreed to within ±6.8%.

relative to P-esters (Diaz *et al*., 2018, 2019). Moreover, *R*. *pomeroyi* is not a significant component of the microbial communities in the Sargasso Sea or Indian Ocean regions where preferential polyP utilization was found (Martin *et al*., 2018). Indeed, we hypothesize that oligotrophs may have a stronger preference for polyP than *R*. *pomeroyi*, which is a copiotroph typically found in high carbon, high nutrient coastal zones. This potential ecosystem-driven adaptation would suggest community-level dynamics in DOP preference that may shape the DOP pool differently in functionally distinct ocean regions; however, further research is needed to reconcile this hypothesis with the uniform DOP compositions reported previously across diverse ocean environments (Young and Ingall, 2010). Yet overall, the capacity of *R*. *pomeroyi* to utilize DOP (Sebastian and Ammerman, 2011) suggests a functional advantage underscoring the importance of DOP as a nutritional resource for microorganisms adapted to ocean regions that are not typically thought of as P limited. This observation is in agreement with studies noting that DOP is actively cycled in coastal zones (Benitez-Nelson and Buesseler, 1999; Alexander *et al*., 2015; Nausch *et al*., 2018).

Within marine microbial communities, DOP acquisition is mediated via two general pathways, which may coexist in the same organism (Li *et al*., 2015; Luo *et al*., 2017; Zhang *et al*., 2017): (i) the extracellular hydrolysis of DOP by cell surface or cell-free P hydrolases and subsequent uptake of Pi and/or (ii) the uptake of low-molecular-weight (<600 Da) DOP (Weiss *et al*., 1991) and subsequent intracellular hydrolysis of Pi. Unlike the majority of DOP sources investigated here, 45polyP is a relatively large molecule (>3 kDa) that is likely to be utilized by extracellular P hydrolases, such as APs and nucleotidases, which are thought to target P-monoesters and nucleotides, respectively. To determine potential enzymes involved in exogenous polyP utilization by *R*. *pomeroyi*, we investigated active cell-free P-hydrolases that were partially isolated from cultures via filtration. Proteomic results revealed the presence of three P-hydrolases across all replicates and media types, including two APs (PhoX and PhoD) and one nucleotidase (5′-NT). We observed significant upregulation of these enzymes under −P conditions (Fig. 5), consistent with the observed upregulation of DOP hydrolysis rates (Fig. 2B–D). The results for 5′-NT are not consistent with previous field investigations, which showed that 5′-NT activity is unaffected by Pi concentrations (Ammerman and Azam, 1985). This inconsistency may reflect fundamental differences in community- versus species-level regulation of 5′-NT expression and/or activity. On the other hand, APA is inhibited by Pi (Dyhrman and Ruttenberg, 2006; Mahaffey *et al*., 2014), which is consistent with our results. Indeed, AP expression is thought to

be transcriptionally regulated by Pi (Dyhrman, 2016). Yet the inhibition of cell-free APA by Pi (Fig. S4) indicates that enzyme-level product inhibition may also play a role, in agreement with pure enzymes studies (Dean, 2002; Zhang *et al*., 2004). Beyond the APs and 5′-NT, we did not observe any polyP-specific intracellular enzymes such as ppk1 or ppk2, which catalyze the synthesis (forward reaction) and degradation (reverse reaction) of polyP (Parnell *et al*., 2018), or ppx, which degrades polyP. Although these genes are more dominant in Pi limited ocean waters and are thought to drive dynamic polyP cycling in those regions (Temperton *et al*., 2011), our results suggest that ppk and ppx may not be involved in the extracellular hydrolysis of polyP. Yet this finding does not rule out the possibility that low-molecular-weight polyP sources may be small enough to be taken up directly and hydrolyzed by intracellular enzymes such as ppk or ppx.

Given the presence of the common P-hydrolases AP and 5′-NT in our dataset, and the absence of any polyP-specific enzymes, we hypothesize that known P-hydrolases may be involved in polyP cycling via broad substrate versatility, in agreement with previous work illustrating broad DOP substrate utilization by a bacterial marine AP (Srivastava *et al*., 2021). To evaluate this hypothesis, we examined the ability of various DOP substrates to compete with the probe MUF-P for reaction with APs from *R. pomeroyi*. Results revealed inhibition of MUF-P hydrolysis by all DOP substrates tested, confirming that *R. pomeroyi* APs have broad substrate versatility (Fig. 6). Consistent with a previous study (Sebastian and Ammerman, 2011) we observed that the P-monoester AMP exhibited the greatest degree of competition against MUF-P, which is expected based on the structural similarity between these two molecules. In further agreement with this prior study, ATP also strongly outcompeted MUF-P hydrolysis. Of the two polyPs tested, 45polyP showed roughly equivalent levels of inhibition as ATP, suggesting a relatively strong affinity of *R. pomeroyi* AP for 45polyP (Fig. S4). In contrast, 3polyP showed the weakest impact on MUF-P hydrolysis, suggesting that *R. pomeroyi* APs have a greater affinity for 45polyP than 3polyP (Fig. S4). This chain length dependence contradicts hydrolysis results from the bulk culture (Fig. 4A), in which 3polyP was preferentially degraded over 45polyP. Together these results suggest that AP is not the only enzyme involved in polyP degradation. For example, the 5′-NT may play a role in polyP cycling and if so, may potentially account for this discrepancy.

Our results on AP-dependent polyP degradation support a previously hypothesized pathway of polyP cycling in the field. For example, Martin *et al*. (2018) observed interbasin differences in polyP content and APA (Diaz *et al*., 2016; Martin *et al*., 2018), leading to the hypothesis that APA exerts a strong degree of control over polyP recycling in marine systems. Indeed, previous studies of pure enzymes also support this hypothesis by showing that APs from calf intestine and *Escherichia coli* exhibit strong reactivity toward polyP, including chain length-dependent hydrolysis by some APs (Lorenz and Schröder, 2001; Sharma *et al*., 2014; Rader, 2017). However, the potential involvement of AP in marine polyP cycling does not necessarily rule out contributions from other enzymes like 5′-NT, as suggested here. Additionally, studies of polyP utilization in cultures of the diatom *Thalassiosira* spp. revealed that APs may not be involved in polyP degradation and that alternative enzymes likely play a role (Diaz *et al*., 2018). Taken together, these lines of evidence suggest that mechanisms of polyP utilization are diverse and dependent on organism functional capacity and polyP chain length.

Overall, this study demonstrates that inorganic polyP is a bioavailable nutritional P resource for *R. pomeroyi*, which supports equivalent levels of growth as model P-monoesters, regardless of chain length. Yet underlying hydrolysis kinetics reveal substantial chain length dependencies in the mechanism, rate and regulation of polyP utilization by *R. pomeroyi*. Therefore, results from this study suggest that microbes control the composition of natural polyP by degrading it in a polymer size-dependent manner. The true composition of natural polyP in seawater reflects a balance of microbial production and degradation processes. Yet, the composition of marine polyP remains largely uncharacterized. Future studies should consider supporting an effort to characterize the range of inorganic polyP chain lengths in marine systems. Due to the roles of polyP in geologic P sequestration (Diaz *et al*., 2008; Huang *et al*., 2018; Wan *et al*., 2019a, 2019b, 2021) and microbial nutritional physiology, a greater understanding of the molecules that make up the polyP component of particulate and dissolved marine P pools may have larger implications for marine P cycling, DOM biogeochemistry and ecosystem functioning.

Experimental procedures

Culture conditions and growth tracking

Ruegeria pomeroyi DSS-3 was cultured in media modified from the recipe of Rivers *et al*. (2016). Briefly, media (100 ml) were prepared using 0.2 μm-filtered natural seawater collected from the Scripps Institution of Oceanography pier that was autoclaved (121°C, 20 min) in 125 ml acid-washed glass Erlenmeyer flasks. Sterile-filtered (0.2 μm) glucose and nutrient stocks, including P sources, were aseptically added to the sterile seawater base in a laminar flow hood. Phosphate-replete media (+Pi) contained 18 μM P. P depleted media (−P) were

prepared by adding phosphate to a final concentration of 1.8 μM P. ATP (Millipore Sigma), AMP (Fisher Scientific), 3polyP (Millipore Sigma), or 45polyP (Millipore Sigma) were added to −P media at a final concentration of 18 μM P. All media were inoculated with 50 μl of *R. pomeroyi* grown to stationary phase in +Pi media, in order to limit the carryover of P. Cultures were grown in a Thermo shaker/incubator at 30°C with shaking at 150 rpm for 10 days. Samples for optical density (600 nm) and flow cytometry were taken daily. Flow cytometry samples were prepared by sampling 2 ml of cultures into cryovials, preserved with a final concentration of 0.5% glutaraldehyde at 4°C for 10 min, and frozen at −80°C until analysis. Growth rates were calculated over the interval of log-linear growth in +Pi cultures. Growth rates in −P cultures were calculated over the same time period as +Pi cultures. All growth experiments were performed in triplicate.

DOP hydrolysis

DOP hydrolysis rates were determined by following the production of Pi, as described previously (Diaz *et al*., 2018, 2019). *Ruegeria pomeroyi* culture samples were collected at the same time from both +Pi and −P media, according to the time period of midlog and stationary phases for +Pi cultures. Two types of samples were prepared from each culture. First, whole culture samples were diluted 1:10 or 1:20 with sterile-filtered (0.2 μm) natural seawater (Diaz *et al*., 2019). Second, cultures were filtered (0.22 μm) in order to generate the cell-free filtrates. Diluted whole culture and filtrate samples were then added to clear 96-well plates and amended with the DOP sources ATP, AMP, 3polyP, 45polyP, or MUF-P (18 μM, final molecular concentration) or Pi (18 μM, final). Briefly, Pi was quantified as soluble reactive phosphorus following the method of Hansen and Koroleff (1999) using a multimode plate reader (Molecular Devices) with a detection limit of 800 nmol L^{-1} P (Diaz *et al*., 2018). Samples were reacted at 4–6 specific timepoints up to 24 h. Each Pi measurement that was derived from a diluted whole culture sample was corrected for cellular Pi uptake as described previously (Diaz *et al*., 2019), and hydrolysis rates were calculated as the slope of Pi production over time using a simple linear regression (typically $R^2 > 0.95$). Hydrolysis rates in diluted whole culture samples were corrected for dilution after regression analysis. To assess abiotic DOP hydrolysis, culture samples were filtered (0.2 μm) and boiled (99°C, 15 min). DOP hydrolysis in these controls was negligible.

APA competition plates

APA was assessed at midlog and stationary phases in undiluted whole culture samples and cell-free filtrates in the presence and absence of DOP sources by following hydrolysis of the fluorogenic substrate MUF-P (Millipore Sigma). MUF-P hydrolysis was tracked using a multimode plate reader (Molecular Devices), using 359 and 449 nm as the excitation and emission wavelengths respectively. Final molecular concentrations of DOP substrates were 0–100 μM (Pi as a control, ATP, AMP, 3polyP and 45polyP). The final concentration of MUF-P was 10 μM. Experiments were run in kinetic mode for 15 min collecting data every 30 s. Enzyme activity was calculated as a percentage of the control hydrolysis rate (no DOP added) to illustrate inhibition of MUF-P by the unlabelled DOP substrates. IC_{50} values for each inhibiting DOP substrate were calculated from the linear regression of log normalized substrate concentrations versus the percent inhibition of MUF-P by each substrate (R^2 typically >0.90). IC_{50} values were calculated according to the formula: $IC_{50} = (0.5\text{-}b)/a$, where b is the y-intercept and a is the slope of the linear regression.

Flow cytometry

For cell counts, culture samples were preserved in filtered (0.22 μm) glutaraldehyde (0.5% final concentration), left to fix at 4°C for 10 min, and frozen at −80°C until analysis. Preserved samples were thawed and counted on a Guava EasyCyte HT flow cytometer (Millipore), and instrument calibration was performed using instrument-specific beads (Luminex). Prior to running on the flow cytometer, samples were prepared in clear, round-bottom 96 well plates (Fisher Scientific) and diluted with filtered (0.22 μm) seawater either 100× (T0, T1) or 1000× (T2–T8). Triplicate blanks prepared with filtered (0.22 μm) seawater and glutaraldehyde (0.5% final concentration) were run with samples, and the average blank cell count was subtracted from all samples. Blanks and diluted samples were stained with diluted SYBR Green nucleic acid gel stain (diluted in deionized water to 100×; Fisher Scientific) and left in the dark for 30 min. After staining, bacterial cell concentrations were analysed at a low flow rate (0.24 μl s^{-1}) for 3 min, and cells were counted based on diagnostic forward scatter versus green fluorescence signals.

Proteomics

To generate samples for exoproteome analysis, +Pi and −P cultures were sampled in stationary phase. Cultures were filtered (0.2 μm), and cell-free filtrates (200 ml) were concentrated (0.5 ml) and exchanged twice into 5 mM Tris (pH 8.0) using a 10 kDa Centricon Plus-70 centrifugal filtration device (Millipore Sigma). Total protein concentrations were determined using a Bradford Protein Assay Kit (Bio-Rad), and concentrated exoproteome

samples were processed with a tryptic in-solution digestion kit (Thermo Scientific), following the manufacturer's instructions. Tryptic peptides were desalted prior to analysis with Pierce C-18 spin columns (Thermo) following the manufacturer's instructions.

Peptide samples were analyzed at the Proteomics and Mass Spectrometry (PAMS) facility at the University of Georgia on a Thermo-Fisher LTQ Orbitrap Elite mass spectrometer coupled with a Proxeon Easy NanoLC system (Waltham, MA, USA). Enzymatic peptides were loaded into a reversed-phase column (self-packed column/emitter with 200 Å 5 μM Bruker MagicAQ C18 resin) and directly eluted into the mass spectrometer. Briefly, the two-buffer gradient elution, following Diaz *et al*. (2018) (0.1% formic acid as buffer A and 99.9% acetonitrile with 0.1% formic acid as buffer B), starts with 5% B, holds at 5% B for 2 min, then increases to 25% B in 60 min, to 40% B in 10 min, and to 95% B in 10 min.

Xcalibur software (version 2.2, Thermo Fisher Scientific) was used for data-dependent acquisition of MS data. A survey MS scan was acquired first, and then the top five ions in the MS scan were selected following collision-induced dissociation and higher-energy collisional dissociation MS/MS analysis. Both MS and MS/MS scans were acquired by the Orbitrap mass spectrometer at resolutions of 120 000 and 30 000 respectively, following Diaz *et al*. (2018).

Protein identification was performed using Thermo Proteome Discoverer (version 1.4) with Mascot (Matrix Science). The reference database consisted of the translated whole genome of *R. pomeroyi* (NCBI Bioproject PRJNA281) (Moran *et al*., 2004; Moran *et al*., 2007; Rivers *et al*., 2014) amended with a list of common contaminants, such as human keratin. Databases included a reversed 'decoy' version for false discovery rate (FDR) analysis. The FDR of identified peptides was ~1%. Finally, in order to determine the relative abundances of proteins under +Pi and −P conditions, the peak area of each protein was normalized to the total protein content in the sample, reported as arbitrary units (A.U.), and the average of three replicates was calculated for each protein of interest.

BLASTP analysis

The *R. pomeroyi* DSS-3 genome was searched for a variety of query sequences from Protein Data Bank (PDB; https://www.rcsb.org) using the National Center for Biotechnology Information (NCBI) online BLASTP suite with default parameters (https://blast.ncbi.nlm.nih.gov). Query sequences included the polyP specific intracellular enzymes: bacterial ppk1 and ppk2 from *E. coli* and *Francisella tularensis* respectively. PDB IDs for query sequences: ppk1: 1XDO, ppk2: 5LLB and ppx: 2FLO.

Statistical analyses

Statistical analyses were performed in JMP Pro (15.2.0). Growth yields, growth rates, DOP hydrolysis and upregulation (fold change) were compared using repeated-measures ANOVA followed by Tukey's Honest significant difference (HSD) test. Protein abundances were compared using Student's *t*-test. *p*-values <0.05 were considered significantly different.

Acknowledgements

The authors acknowledge Alisia Holland for contributing to the development of culturing methods during an early stage of this project. This work was supported by the National Science Foundation under grants 1737083, 2001212 (S.D.), 1736967, 1948042 (J.M.D.), 1737240 (S.D.), 1559124 and 2015310 (J.M.D.), as well as the Simons Foundation under grant 678537 (J.M.D.) and the Sloan Foundation (J.M.D.). The raw data supporting the conclusions of this manuscript are deposited at the Biological and Chemical Oceanography Data Management Office (http://bco-dmo.org) under project number 747715.

References

Alexander, H., Jenkins, B.D., Rynearson, T.A., and Dyhrman, S.T. (2015) Metatranscriptome analyses indicate resource partitioning between diatoms in the field. *Proc Natl Acad Sci U S A* **112**: E2182. https://doi.org/10.1073/pnas.1421993112.

Ammerman, J.W., and Azam, F. (1985) Bacterial 5-nucleotidase in aquatic ecosystems: a novel mechanism of phosphorus regeneration. *Science* **227**: 1338. https://doi.org/10.1126/science.227.4692.1338.

Benitez-Nelson, C.R., and Buesseler, K.O. (1999) Variability of inorganic and organic phosphorus turnover rates in the coastal ocean. *Nature* **398**: 502–505. https://doi.org/10.1038/19061.

Björkman, K., and Karl, D. (1994) Bioavailability of inorganic and organic phosphorus compounds to natural assemblages of microorganisms in Hawaiian coastal waters. *Mar Ecol Prog Ser* **111**: 265–273.

Björkman, K., and Karl, D. (2005) Presence of dissolved nucleotides in the North Pacific Subtropical Gyre and their role in cycling of dissolved organic phosphorus. *Aquat Microb Ecol* **39**: 193–203. https://doi.org/10.3354/ame039193.

Buchan, A., González, J.M., and Moran, M.A. (2005) Overview of the marine roseobacter lineage. *Appl Environ Microbiol* **71**: 5665–5677. https://doi.org/10.1128/AEM.71.10.5665-5677.2005.

Cui, Y., Lin, X., Zhang, H., Lin, L., and Lin, S. (2016) PhnW-PhnX pathway in dinoflagellates not functional to utilize extracellular phosphonates. *Front Mar Sci* **2**: 120. https://doi.org/10.3389/fmars.2015.00120.

Davis, C.E., and Mahaffey, C. (2017) Elevated alkaline phosphatase activity in a phosphate-replete environment: influence of sinking particles. *Limnol Oceanogr* **62**: 2389–2403. https://doi.org/10.1002/lno.10572.

Dean, R.L. (2002) Kinetic studies with alkaline phosphatase in the presence and absence of inhibitors and divalent

cations. *Biochem Mol Biol Educ* **30**: 401–407. https://doi.org/10.1002/bmb.2002.494030060138.

Diaz, J., Ingall, E., Benitez-Nelson, C., Paterson, D., de Jonge, M.D., McNulty, I., and Brandes, J.A. (2008) Marine polyphosphate: a key player in geologic phosphorus sequestration. *Science* **320**: 652. https://doi.org/10.1126/science.1151751.

Diaz, J.M., Björkman, K.M., Haley, S.T., Ingall, E.D., Karl, D. M., Longo, A.F., *et al*. (2016) Polyphosphate dynamics at Station ALOHA, North Pacific subtropical gyre. *Limnol Oceanogr* **61**: 227–239. https://doi.org/10.1002/lno.10206.

Diaz, J.M., Holland, A., Sanders, J.G., Bulski, K., Mollett, D., Chou, C.-W., *et al*. (2018) Dissolved organic phosphorus utilization by phytoplankton reveals preferential degradation of polyphosphates over Phosphomonoesters. *Front Mar Sci* **5**: 380. https://doi.org/10.3389/fmars.2018.00380.

Diaz, J.M., and Ingall, E.D. (2010) Fluorometric quantification of natural inorganic polyphosphate. *Environ Sci Technol* **44**: 4665–4671. https://doi.org/10.1021/es100191h.

Diaz, J.M., Steffen, R., Sanders, J.G., Tang, Y., and Duhamel, S. (2019) Preferential utilization of inorganic polyphosphate over other bioavailable phosphorus sources by the model diatoms *Thalassiosira* spp. *Environ Microbiol* **21**: 2415–2425. https://doi.org/10.1111/1462-2920.14630.

Duhamel, S., Diaz, J.M., Adams, J.C., Djaoudi, K., Steck, V., and Waggoner, E.M. (2021) Phosphorus as an integral component of global marine biogeochemistry. *Nat Geosci* **14**: 359–368. https://doi.org/10.1038/s41561-021-00755-8.

Dyhrman, S.T. (2016) Nutrients and their acquisition: phosphorus physiology in microalgae. In *The Physiology of Microalgae*, Borowitzka, M.A., Beardall, J., and Raven, J.A. (eds): Cham, Switzerland: Springer International Publishing, pp. 155–183. https://doi.org/10.1007/978-3-319-24945-2_8.

Dyhrman, S.T., and Ruttenberg, K.C. (2006) Presence and regulation of alkaline phosphatase activity in eukaryotic phytoplankton from the coastal ocean: implications for dissolved organic phosphorus remineralization. *Limnol Oceanogr* **51**: 1381–1390. https://doi.org/10.4319/lo.2006.51.3.1381.

Hansen, H.P., and Koroleff, F. (1999) Determination of nutrients. In *Methods of Seawater Analysis*: Weinheim, Germany: John Wiley & Sons, pp. 159–228. https://doi.org/10.1002/9783527613984.ch10.

Huang, R., Wan, B., Hultz, M., Diaz, J.M., and Tang, Y. (2018) Phosphatase-mediated hydrolysis of linear polyphosphates. *Environ Sci Technol* **52**: 1183–1190. https://doi.org/10.1021/acs.est.7b04553.

Karl, D., and Björkman, K. (2015) Dynamics of dissolved organic phosphorus. In *Biogeochemistry of Marine Dissolved Organic Matter*, 2nd ed, pp. 233–334. London: Academic Press. https://doi.org/10.1016/B978-0-12-405940-5.00005-4.

Karl, D.M. (2014) Microbially mediated transformations of phosphorus in the sea: new views of an old cycle. *Ann Rev Mar Sci* **6**: 279–337. https://doi.org/10.1146/annurev-marine-010213-135046.

Kornberg, A., Rao, N.N., and Ault-Riché, D. (1999) Inorganic polyphosphate: a molecule of many functions. *Annu Rev Biochem* **68**: 89–125. https://doi.org/10.1146/annurev.biochem.68.1.89.

Letscher, R.T., and Moore, J.K. (2015) Preferential remineralization of dissolved organic phosphorus and non-Redfield DOM dynamics in the global ocean: impacts on marine productivity, nitrogen fixation, and carbon export. *Global Biogeochem Cycles* **29**: 325–340. https://doi.org/10.1002/2014GB004904.

Li, M., Li, L., Shi, X., Lin, L., and Lin, S. (2015) Effects of phosphorus deficiency and adenosine 5′-triphosphate (ATP) on growth and cell cycle of the dinoflagellate *Prorocentrum donghaiense*. *Harmful Algae* **47**: 35–41.

Lin, S., Wayne Litaker, R., and Sunda, W.G. (2016) Phosphorus physiological ecology and molecular mechanisms in marine phytoplankton. *J Phycol* **52**: 10–36.

Lorenz, B., and Schröder, H.C. (2001) Mammalian intestinal alkaline phosphatase acts as highly active exopolyphosphatase. *Biochim Biophys Acta (BBA) - Protein Struct Mol Enzymol* **1547**: 254–261. https://doi.org/10.1016/S0167-4838(01)00193-5.

Luo, H., Lin, X., Li, L., Lin, L., Zhang, C., and Lin, S. (2017) Transcriptomic and physiological analyses of the dinoflagellate *Karenia mikimotoi* reveal non-alkaline phosphatase-based molecular machinery of ATP utilisation. *Environ Microbiol* **19**: 4506–4518.

Mahaffey, C., Reynolds, S., Davis, C.E., and Lohan, M.C. (2014) Alkaline phosphatase activity in the subtropical ocean: insights from nutrient, dust and trace metal addition experiments. *Front Mar Sci* **1**: 73. https://doi.org/10.3389/fmars.2014.00073.

Martin, P., Dyhrman, S.T., Lomas, M.W., Poulton, N.J., and Van Mooy, B.A.S. (2014) Accumulation and enhanced cycling of polyphosphate by Sargasso Sea plankton in response to low phosphorus. *Proc Natl Acad Sci U S A* **111**: 8089. https://doi.org/10.1073/pnas.1321719111.

Martin, P., Lauro, F.M., Sarkar, A., Goodkin, N., Prakash, S., and Vinayachandran, P.N. (2018) Particulate polyphosphate and alkaline phosphatase activity across a latitudinal transect in the tropical Indian Ocean. *Limnol Oceanogr* **63**: 1395–1406. https://doi.org/10.1002/lno.10780.

Martin, P., and Van Mooy, B.A.S. (2013) Fluorometric quantification of polyphosphate in environmental plankton samples: extraction protocols, matrix effects, and nucleic acid interference. *Appl Environ Microbiol* **79**: 273–281. https://doi.org/10.1128/AEM.02592-12.

Moore, L.R., Ostrowski, M., Scanlan, D.J., Feren, K., and Sweetsir, T. (2005) Ecotypic variation in phosphorus-acquisition mechanisms within marine picocyanobacteria. *Aquat Microb Ecol* **39**: 257–269.

Moran, M.A., Belas, R., Schell, M.A., González, J.M., Sun, F., Sun, S., *et al*. (2007) Ecological genomics of marine roseobacters. *Appl Environ Microbiol* **73**: 4559–4569. https://doi.org/10.1128/AEM.02580-06.

Moran, M.A., Buchan, A., González, J.M., Heidelberg, J.F., Whitman, W.B., Kiene, R.P., *et al*. (2004) Genome sequence of Silicibacter pomeroyi reveals adaptations to the marine environment. *Nature* **432**: 910–913. https://doi.org/10.1038/nature03170.

Nausch, M., Achterberg, E.P., Bach, L.T., Brussaard, C.P. D., Crawfurd, K.J., Fabian, J., *et al*. (2018) Concentrations and uptake of dissolved organic phosphorus compounds in the Baltic sea. *Front Mar Sci* **5**: 386. https://doi.org/10.3389/fmars.2018.00386.

Parnell, A.E., Mordhorst, S., Kemper, F., Giurrandino, M., Prince, J.P., Schwarzer, N.J., *et al*. (2018) Substrate

recognition and mechanism revealed by ligand-bound polyphosphate kinase 2 structures. *Proc Natl Acad Sci U S A* **115**: 3350. https://doi.org/10.1073/pnas.1710741115.

Paytan, A., Cade-Menun, B.J., McLaughlin, K., and Faul, K. L. (2003) Selective phosphorus regeneration of sinking marine particles: evidence from 31P-NMR. *Mar Chem* **82**: 55–70. https://doi.org/10.1016/S0304-4203(03)00052-5.

Posacka, A.M., Semeniuk, D.M., and Maldonado, M.T. (2019) Effects of copper availability on the physiology of marine heterotrophic bacteria. *Front Mar Sci* **5**: 523. https://doi.org/10.3389/fmars.2018.00523.

Rader, B.A. (2017) Alkaline phosphatase, an unconventional immune protein. *Front Immunol* **8**: 897. https://doi.org/10.3389/fimmu.2017.00897.

Repeta, D.J., Ferrón, S., Sosa, O.A., Johnson, C.G., Repeta, L.D., Acker, M., *et al*. (2016) Marine methane paradox explained by bacterial degradation of dissolved organic matter. *Nat Geosci* **9**: 884–887. https://doi.org/10.1038/ngeo2837.

Rivers, A.R., Burns, A.S., Chan, L.-K., and Moran, M.A. (2016) Experimental identification of small non-coding RNAs in the model marine bacterium *Ruegeria pomeroyi* DSS-3. *Front Microbiol* **7**: 380. https://doi.org/10.3389/fmicb.2016.00380.

Rivers, A.R., Smith, C.B., and Moran, M.A. (2014) An updated genome annotation for the model marine bacterium *Ruegeria pomeroyi* DSS-3. *Stand Genomic Sci* **9**: 11. https://doi.org/10.1186/1944-3277-9-11.

Sannigrahi, P., and Ingall, E. (2005) Polyphosphates as a source of enhanced P fluxes in marine sediments overlain by anoxic waters: evidence from 31P NMR. *Geochem Trans* **6**: 52. https://doi.org/10.1186/1467-4866-6-52.

Sebastian, M., and Ammerman, J.W. (2011) Role of the phosphatase PhoX in the phosphorus metabolism of the marine bacterium *Ruegeria pomeroyi* DSS-3. *Environ Microbiol Rep* **3**: 535–542. https://doi.org/10.1111/j.1758-2229.2011.00253.x.

Sharma, U., Pal, D., and Prasad, R. (2014) Alkaline phosphatase: an overview. *Indian J Clin Biochem* **29**: 269–278. https://doi.org/10.1007/s12291-013-0408-y.

Sosa, O.A., Burrell, T.J., Wilson, S.T., Foreman, R.K., Karl, D.M., and Repeta, D.J. (2020) Phosphonate cycling supports methane and ethylene supersaturation in the phosphate-depleted western North Atlantic Ocean. *Limnol Oceanogr* **65**: 2443–2459. https://doi.org/10.1002/lno.11463.

Sosa, O.A., Repeta, D.J., DeLong, E.F., Ashkezari, M.D., and Karl, D.M. (2019) Phosphate-limited ocean regions select for bacterial populations enriched in the carbon–phosphorus lyase pathway for phosphonate degradation. *Environ Microbiol* **21**: 2402–2414. https://doi.org/10.1111/1462-2920.14628.

Srivastava, A., Saavedra, D.E.M., Thomson, B., García, J.A. L., Zhao, Z., Patrick, W.M., *et al*. (2021) Enzyme promiscuity in natural environments: alkaline phosphatase in the ocean. *ISME J* **15**: 3375–3383. https://doi.org/10.1038/s41396-021-01013-w.

Temperton, B., Gilbert, J.A., Quinn, J.P., and McGrath, J.W. (2011) Novel analysis of oceanic surface water metagenomes suggests importance of polyphosphate metabolism in oligotrophic environments. *PLoS One* **6**: e16499. https://doi.org/10.1371/journal.pone.0016499.

Wan, B., Huang, R., Diaz, J.M., and Tang, Y. (2019a) Polyphosphate adsorption and hydrolysis on aluminum oxides. *Environ Sci Technol* **53**: 9542–9552. https://doi.org/10.1021/acs.est.9b01876.

Wan, B., Huang, R., Diaz, J.M., and Tang, Y. (2019b) Manganese oxide catalyzed hydrolysis of polyphosphates. *ACS Earth Space Chem* **3**: 2623–2634. https://doi.org/10.1021/acsearthspacechem.9b00220.

Wan, B., Yang, P., Jung, H., Zhu, M., Diaz, J.M., and Tang, Y. (2021) Iron oxides catalyze the hydrolysis of polyphosphate and precipitation of calcium phosphate minerals. *Geochim Cosmochim Acta* **305**: 49–65. https://doi.org/10.1016/j.gca.2021.04.031.

Wang, C., Lin, X., Li, L., and Lin, S. (2016) Differential growth responses of marine phytoplankton to herbicide glyphosate. *PLoS One* **11**: e0151633. https://doi.org/10.1371/journal.pone.0151633.

Weiss, M.S., Abele, U., Weckesser, J., Welte, W., Schiltz, E., and Schultz, G.E. (1991) Molecular architecture and electrostatic properties of a bacterial porin. *Science* **254**: 1627–1630.

White, A., Watkins-Brandt, K., Engle, M., Burkhardt, B., and Paytan, A. (2012) Characterization of the rate and temperature sensitivities of bacterial remineralization of dissolved organic phosphorus compounds by natural populations. *Front Microbiol* **3**: 276. https://doi.org/10.3389/fmicb.2012.00276.

Whitney, L.P., and Lomas, M.W. (2019) Phosphonate utilization by eukaryotic phytoplankton. *Limnol Oceanogr Lett* **4**: 18–24. https://doi.org/10.1002/lol2.10100.

Young, C.L., and Ingall, E.D. (2010) Marine dissolved organic phosphorus composition: insights from samples recovered using combined electrodialysis/reverse osmosis. *Aquat Geochem* **16**: 563–574. https://doi.org/10.1007/s10498-009-9087-y.

Zhang, C., Luo, H., Huang, L., and Lin, S. (2017) Molecular mechanism of glucose-6-phosphate utilization in the dinoflagellate *Karenia mikimotoi*. *Harmful Algae* **67**: 74–84.

Zhang, L., Buchet, R., and Azzar, G. (2004) Phosphate binding in the active site of alkaline phosphatase and the interactions of 2-nitrosoacetophenone with alkaline phosphatase-induced small structural changes. *Biophys J* **86**: 3873–3881. https://doi.org/10.1529/biophysj.103.034116.

Zimmerman, A.E., Allison, S.D., and Martiny, A.C. (2014) Phylogenetic constraints on elemental stoichiometry and resource allocation in heterotrophic marine bacteria. *Environ Microbiol* **16**: 1398–1410. https://doi.org/10.1111/1462-2920.12329.

Supporting Information

Additional Supporting Information may be found in the online version of this article at the publisher's web-site:

Supporting Information Dataset 1. Exoproteome data for *R. pomeroyi* + Pi and −P cultures. A, B, and C indicate biological replicates.

Appendix S1: Supporting Information.